Continuous-domain Sparse Inverse Problems

Quentin Denoyelle

Séminaire Équations aux Dérivées Partielles
IRMA - Université de Strasbourg
22 mars 2022

Université Paris Cité

LABORATOIRE MAP5

Sommaire

Inverse Problems

Measuring devices have a non sharp impulse response : observations are a **blurred** version of a “true ideal scene”.

Application in

- Geophysics,
- Astronomy,
- Microscopy,
- Spectroscopy,
- ...

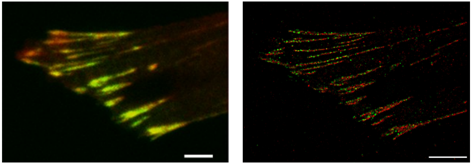

(a) Widefield microscope (b) PALM

FIGURE – *Images obtained from the Cell Image Library*

Goal : Obtain as much detail as we can from given measurements.

Sparse linear inverse problems

FIGURE – 2D and 3D Single Molecule Localization Microscopy (SMLM)

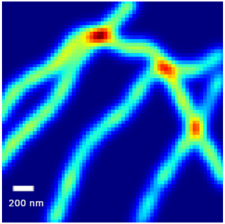

Classical microscope

Sparse linear inverse problems

FIGURE – 2D and 3D Single Molecule Localization Microscopy (SMLM)

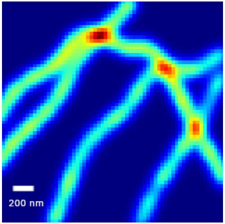

Classical microscope

vs

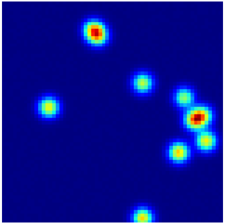

Frame 1

PALM/STORM

Sparse linear inverse problems

FIGURE – 2D and 3D Single Molecule Localization Microscopy (SMLM)

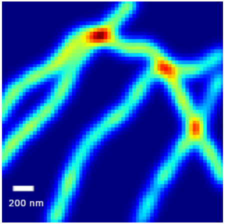

Classical microscope

vs

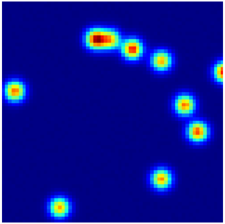

Frame 2

PALM/STORM

Sparse linear inverse problems

FIGURE – 2D and 3D Single Molecule Localization Microscopy (SMLM)

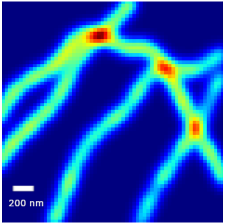

Classical microscope

vs

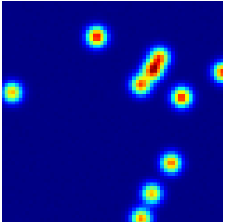

Frame 3...

PALM/STORM

Sparse linear inverse problems

FIGURE – 2D and 3D Single Molecule Localization Microscopy (SMLM)

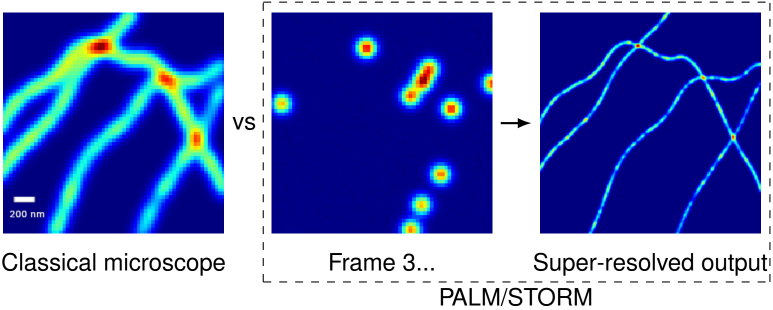

Sparse linear inverse problems

FIGURE – 2D and 3D Single Molecule Localization Microscopy (SMLM)

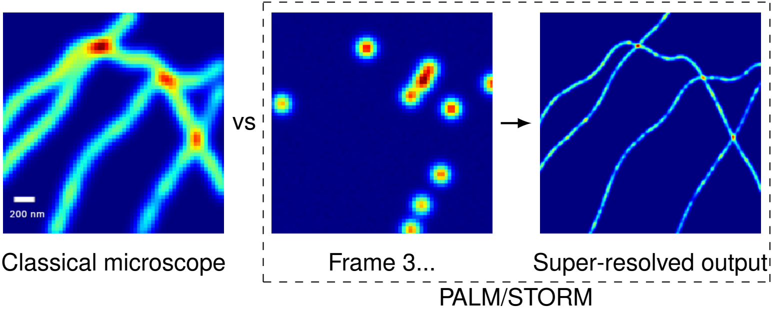

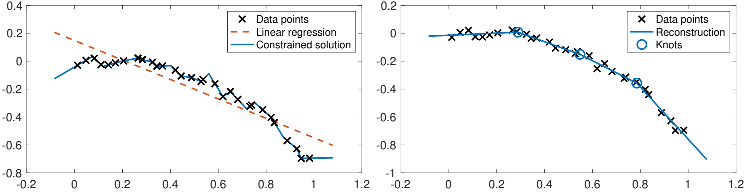

FIGURE – Sparse piecewise-linear representation of data

Model : continuous-domain sparse inverse problem

Input : Sparse Radon measures

$$m_{a_0,x_0} \stackrel{\text{def.}}{=} \sum_{i=1}^{N} a_{0,i}\delta_{x_{0,i}} \quad a_{0,i} \in \mathbb{R},\ x_{0,i} \in \mathcal{X} = \mathbb{R}^d \text{ or } \mathbb{T}^d.$$

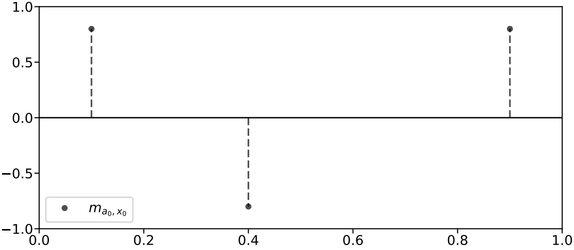

Model : continuous-domain sparse inverse problem

Input : Sparse Radon measures

$$m_{a_0,x_0} \stackrel{\text{def.}}{=} \sum_{i=1}^{N} a_{0,i}\delta_{x_{0,i}} \quad a_{0,i} \in \mathbb{R},\ x_{0,i} \in \mathcal{X} = \mathbb{R}^d \text{ or } \mathbb{T}^d.$$

Forward operator : $\Phi : \mathcal{M}(\mathcal{X}) \to \mathbb{R}^M$ linear continuous, $\mathcal{M}(\mathcal{X})$ space of bounded Radon measures on $\mathcal{X} = \mathbb{T}^d$ or $\mathbb{R}^d$.

Measurements : $y_0 \stackrel{\text{def.}}{=} \Phi m_{a_0,x_0} \in \mathbb{R}^M$

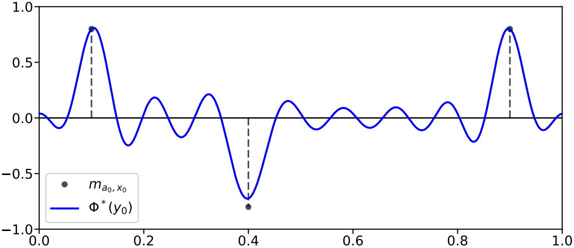

FIGURE – Φ ideal low pass filter.

Model : continuous-domain sparse inverse problem

Input : Sparse Radon measures

$$m_{a_0,x_0} \overset{\text{def.}}{=} \sum_{i=1}^{N} a_{0,i}\delta_{x_{0,i}} \quad a_{0,i} \in \mathbb{R},\ x_{0,i} \in \mathcal{X} = \mathbb{R}^d \text{ or } \mathbb{T}^d.$$

Forward operator : $\Phi : \mathcal{M}(\mathcal{X}) \to \mathbb{R}^M$ linear continuous,
$\mathcal{M}(\mathcal{X})$ space of bounded Radon measures on $\mathcal{X} = \mathbb{T}^d$ or $\mathbb{R}^d$.

Measurements : $y_0 \overset{\text{def.}}{=} \Phi m_{a_0,x_0} \in \mathbb{R}^M$ or $y = y_0 + w \in \mathbb{R}^M$

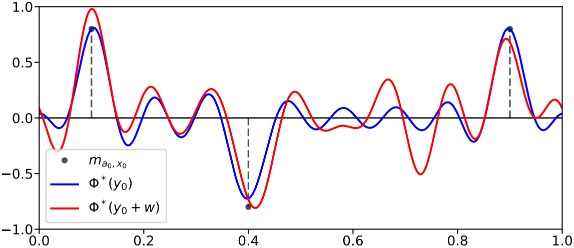

FIGURE – Φ ideal low pass filter.

Model : continuous-domain sparse inverse problem

Input : Sparse Radon measures

$$m_{a_0,x_0} \overset{\text{def.}}{=} \sum_{i=1}^{N} a_{0,i}\delta_{x_{0,i}} \quad a_{0,i} \in \mathbb{R},\ x_{0,i} \in \mathcal{X} = \mathbb{R}^d \text{ or } \mathbb{T}^d.$$

Forward operator : $\Phi : \mathcal{M}(\mathcal{X}) \to \mathbb{R}^M$ linear continuous, $\mathcal{M}(\mathcal{X})$ space of bounded Radon measures on $\mathcal{X} = \mathbb{T}^d$ or $\mathbb{R}^d$.

Measurements : $y_0 \overset{\text{def.}}{=} \Phi m_{a_0,x_0} \in \mathbb{R}^M$ or $y = y_0 + w \in \mathbb{R}^M$

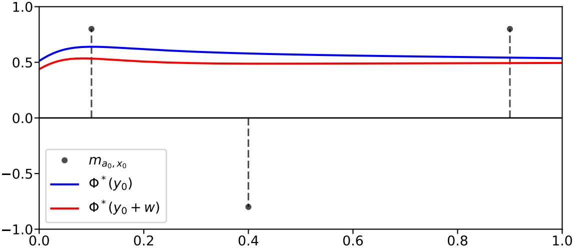

FIGURE – Φ is a discretized Laplace transform.

Model : continuous-domain sparse inverse problem

Input : Sparse Radon measures

$$m_{a_0,x_0} \overset{\text{def.}}{=} \sum_{i=1}^{N} a_{0,i}\delta_{x_{0,i}} \quad a_{0,i} \in \mathbb{R},\ x_{0,i} \in \mathcal{X} = \mathbb{R}^d \text{ or } \mathbb{T}^d.$$

Forward operator : $\Phi : \mathcal{M}(\mathcal{X}) \to \mathbb{R}^M$ linear continuous,
$\mathcal{M}(\mathcal{X})$ space of bounded Radon measures on $\mathcal{X} = \mathbb{T}^d$ or $\mathbb{R}^d$.

Measurements : $y_0 \overset{\text{def.}}{=} \Phi m_{a_0,x_0} \in \mathbb{R}^M$ or $y = y_0 + w \in \mathbb{R}^M$

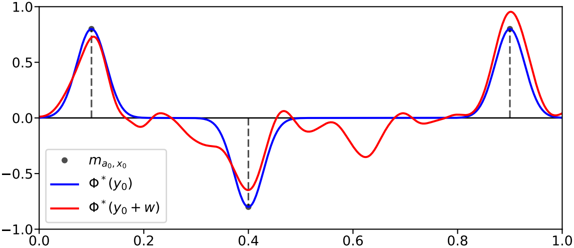

FIGURE – Φ is a convolution with a Gaussian kernel.

Question : recover $m_{\mathbf{a_0},\mathbf{x_0}} \in \mathcal{M}(\mathcal{X})$ from $y \in \mathbb{R}^M$?

Model : continuous-domain sparse inverse problem

Problem : From $y_0 \stackrel{\text{def.}}{=} \Phi m_{a_0,x_0}$

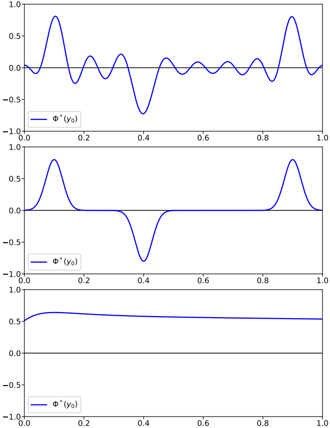

Model : continuous-domain sparse inverse problem

Problem : From $y_0 \stackrel{\text{def.}}{=} \Phi m_{a_0,x_0}$ recover m_{a_0,x_0}

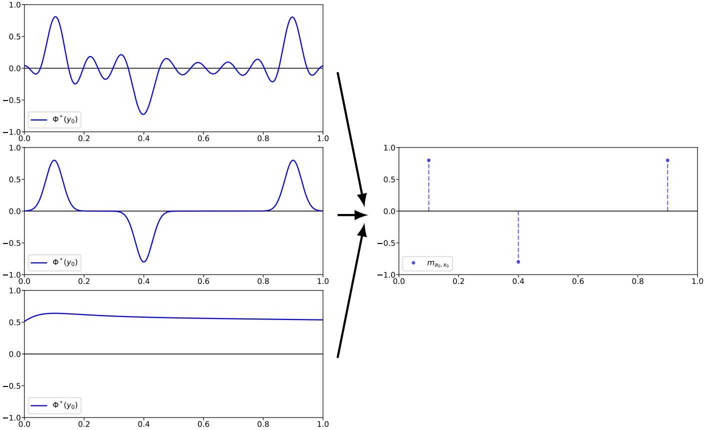

Model : continuous-domain sparse inverse problem

Problem : From $y_0 \stackrel{\text{def.}}{=} \Phi m_{a_0,x_0}$ or $y_0 + w$, recover m_{a_0,x_0} or $m_{a,x}$ "close".

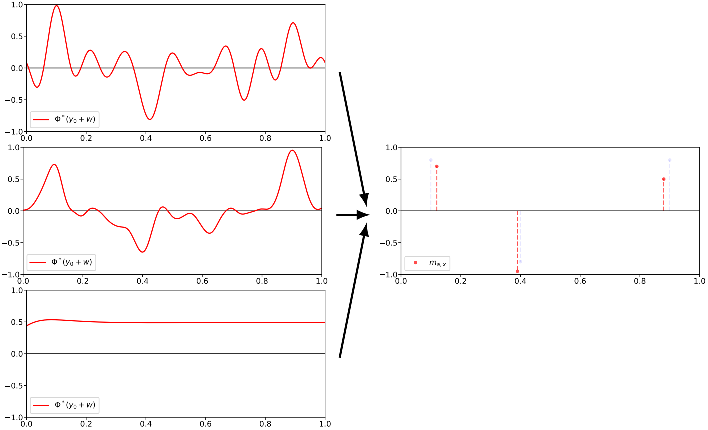

Model : continuous-domain sparse inverse problem

Problem : From $y_0 \stackrel{\text{def.}}{=} \Phi m_{a_0,x_0}$ or $y_0 + w$, recover m_{a_0,x_0} or $m_{a,x}$ "close".

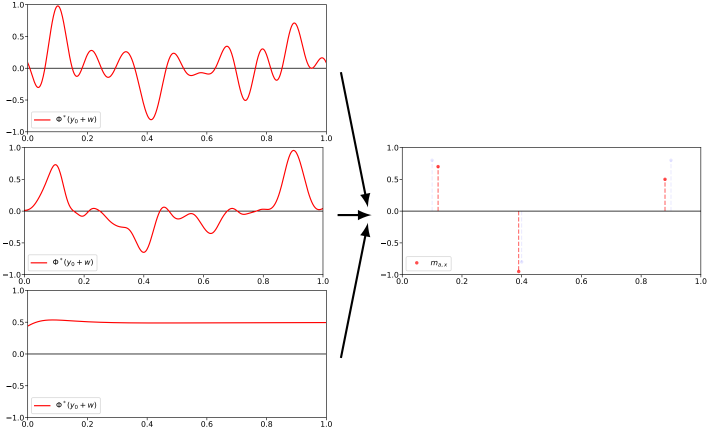

One strategy : Prony's methods (MUSIC, ESPRIT,...)

- Advantages : always works when $w = 0$, insensitive to the sign of the amplitudes.
- Drawbacks : works only for deconvolution.

Grid-free support recovery

Method : Variational approach using low a complexity prior.

Grid-free support recovery

Method : Variational approach using low a complexity prior.

Definition (Total Variation Norm on $\mathcal{M}(\mathcal{X})$)

$$|m|(\mathcal{X}) = \sup\{\int_{\mathcal{X}} \psi \mathrm{d}m : \ \psi \in \mathcal{C}(\mathcal{X}), \|\psi\|_\infty \leq 1\}$$

is total mass of m and extends ℓ_1 *norm for vectors* ($|m_{a_0,x_0}|(\mathcal{X}) = \|a_0\|_1$).

Grid-free support recovery

Method : Variational approach using low a complexity prior.

Definition (Total Variation Norm on $\mathcal{M}(\mathcal{X})$)

$$|m|(\mathcal{X}) = \sup\{\int_{\mathcal{X}} \psi \mathrm{d}m : \ \psi \in \mathcal{C}(\mathcal{X}), \|\psi\|_\infty \leq 1\}$$

is total mass of m and extends ℓ_1 norm for vectors ($|m_{a_0,x_0}|(\mathcal{X}) = \|a_0\|_1$).

Basis Pursuit in the Continuum
(Candès-FG 13', de Castro & al 12')

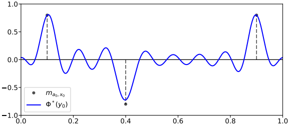

$$\min_{\Phi m = y_0} |m|(\mathcal{X})$$
$$(BPC)$$

BLASSO
(Bredies & al 13', Azais & al 15')

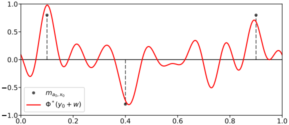

$$\min_{m \in \mathcal{M}} \frac{1}{2}\|\Phi m - (y_0 + w)\|^2 + \lambda |m|(\mathcal{X})$$
$$(BLASSO)$$

Remark :

- No discretization ! Continuous setting.

Achievements of the method

Recovery result for (BPC)

Theorem (Candès-FG 13', FG 16')

If Φ is the ideal low-pass filter and $\Delta(m_{a_0,x_0}) \geq \frac{1{,}26}{f_c}$ where

$$\Delta(m_{a_0,x_0}) \overset{\text{def.}}{=} \min_{i \neq j} |x_{0,i} - x_{0,j}|,$$

then m_{a_0,x_0} is the unique solution to

$$\min_{\Phi m = y_0} |m|(\mathbb{T}) \quad (BPC).$$

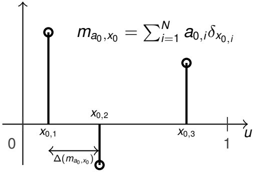

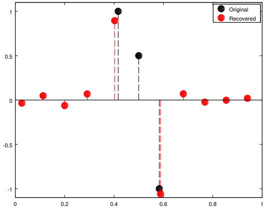

FIGURE – Spikes with different signs too close $\Rightarrow$ reconstruction of m_{a_0,x_0} impossible.

Achievements of the method

Identifiability of Positive Measures for (BPC)

Theorem (de Castro & Gamboa 12')

Φ *ideal low-pass filter, cutoff frequency* f_c.
If m_{a_0,x_0} *has* $N \leq f_c$ *positive Dirac masses, then unique solution of* (BPC).

Achievements of the method

Identifiability of Positive Measures for (BPC)

Theorem (de Castro & Gamboa 12')

Φ *ideal low-pass filter, cutoff frequency* f_c.
If m_{a_0,x_0} *has* $N \leq f_c$ *positive Dirac masses, then unique solution of* (BPC).

Proposition (Certificate)

m_{a_0,x_0} *is a solution of* (BPC) *if there exists* $\eta \in \mathcal{C}(\mathcal{X}) \cap \mathrm{Im}(\Phi^*)$ *satisfying*

$$\forall i, \eta(x_{0,i}) = \mathrm{sign}(a_{0,i}) \quad \textit{and} \quad \|\eta\|_\infty \leq 1.$$

Achievements of the method

Identifiability of Positive Measures for (BPC)

Theorem (de Castro & Gamboa 12')

Φ *ideal low-pass filter, cutoff frequency* f_c.
If m_{a_0,x_0} *has* $N \leq f_c$ *positive Dirac masses, then unique solution of* (BPC).

Démonstration.

The following function

$$\forall u \in \mathbb{T}, \quad \eta(u) = 1 - c \prod_{i=1}^{N} (\sin(\pi(u - x_{0,i})))^2,$$

satisfies $\eta \in \operatorname{Im} \Phi^*$, $\eta(x_{0,i}) = 1$ and $\|\eta\|_\infty \leq 1$ for $c > 0$ small enough. $\square$

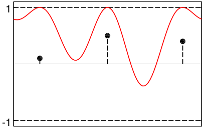

FIGURE – η for 3 spikes.

Proposition (Certificate)

m_{a_0,x_0} *is a solution of* (BPC) *if there exists* $\eta \in \mathcal{C}(\mathcal{X}) \cap \operatorname{Im}(\Phi^*)$ *satisfying*

$$\forall i, \eta(x_{0,i}) = \operatorname{sign}(a_{0,i}) \quad \textit{and} \quad \|\eta\|_\infty \leq 1.$$

Identifiability of Positive Measures for (BPC)

Theorem (de Castro & Gamboa 12')

Φ *ideal low-pass filter, cutoff frequency f_c.*
If m_{a_0,x_0} has $N \leq f_c$ positive Dirac masses, then unique solution of (BPC).

Démonstration.
The following function

$$\forall u \in \mathbb{T}, \quad \eta(u) = 1 - c\prod_{i=1}^{N}(\sin(\pi(u - x_{0,i})))^2,$$

satisfies $\eta \in \operatorname{Im}\Phi^*$, $\eta(x_{0,i}) = 1$ and $\|\eta\|_\infty \leq 1$ for $c > 0$ small enough.

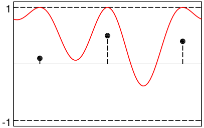

□ FIGURE – η for 3 spikes.

Proposition (Certificate)

m_{a_0,x_0} is a solution of (BPC) if there exists $\eta \in \mathcal{C}(\mathcal{X}) \cap \operatorname{Im}(\Phi^*)$ satisfying

$$\forall i, \eta(x_{0,i}) = \operatorname{sign}(a_{0,i}) \quad \textit{and} \quad \|\eta\|_\infty \leq 1.$$

Consequence : $\Delta(m_{a_0,x_0}) \to 0$, recovery of m_{a_0,x_0} always guarenteed.

Achievements of the Method

Stability to noise

Theorem (Bredies-Pikkarainen 13')

If the solution to (BPC) *is unique then the solutions of*

$$\min_{m \in \mathcal{M}(\mathcal{X})} \frac{1}{2} \|\Phi m - (y_0 + w)\|^2 + \lambda |m|(\mathcal{X}), \quad (BLASSO),$$

converge in the weak- sense, when* $\lambda, \frac{\|w\|^2}{\lambda} \to 0$, *to the solution of* (BPC).

Achievements of the Method

Stability to noise

Theorem (Bredies-Pikkarainen 13')

If the solution to (BPC) *is unique then the solutions of*

$$\min_{m \in \mathcal{M}(\mathcal{X})} \frac{1}{2} \|\Phi m - (y_0 + w)\|^2 + \lambda |m|(\mathcal{X}), \quad (BLASSO),$$

converge in the weak- sense, when* $\lambda, \frac{\|w\|^2}{\lambda} \to 0$*, to the solution of* (BPC)*.*

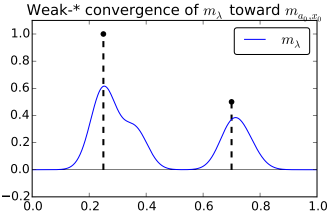

FIGURE – m_λ, sol of $(BLASSO)$, weak-* converges toward m_{a_0,x_0} when $\lambda, \frac{\|w\|^2}{\lambda} \to 0$.

Problem : No information on the structure of m_λ.

Agnostic recovery for (BPC). Uniqueness.

Theorem (de Castro & Gamboa 12')

Φ ideal low-pass filter, cutoff frequency f_c.
If m_{a_0,x_0} has $N \leq f_c$ positive Dirac masses, then unique solution of (BPC).

Framework : $y_0 = \Phi\left(\sum_{i=1}^{N} a_{0,i}\delta_{x_{0,i}}\right)$, with $N \leq f_c$.

Question : what if $y_0 = \Phi(?)$ or $y_0 = \Phi(m_{a_0,x_0})$ with m_{a_0,x_0} not solution.

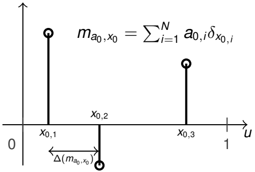

FIGURE – $y_0 = \Phi(m_{a_0,x_0})$, but m_{a_0,x_0} not solution if $\Delta(m_{a_0,x_0})$ small. Exists sparse solution ? Unique ?

Agnostic recovery for (BPC). Uniqueness.

Theorem (de Castro & Gamboa 12')

Φ ideal low-pass filter, cutoff frequency f_c.
If m_{a_0,x_0} has $N \leq f_c$ positive Dirac masses, then unique solution of (BPC).

Framework : $y_0 = \Phi\left(\sum_{i=1}^N a_{0,i}\delta_{x_{0,i}}\right)$, with $N \leq f_c$.

Question : what if $y_0 = \Phi(?)$ or $y_0 = \Phi(m_{a_0,x_0})$ with m_{a_0,x_0} not solution.

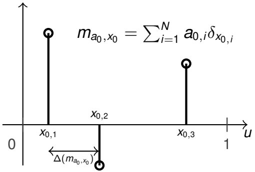

FIGURE – $y_0 = \Phi(m_{a_0,x_0})$, but m_{a_0,x_0} not solution if $\Delta(m_{a_0,x_0})$ small. Exists sparse solution ? Unique ?

Theorem (Unser & al. 17', Boyer & al. 18', Fisher & Jerome 1975, Dubins 1962)

Representer theorem : for all y_0, always exists sparse solution of (BPC) with at most $2f_c + 1$ Dirac masses.

Question : when is it unique ?

Agnostic recovery for (BPC). Uniqueness.

Assumption :

- Φ ideal low pass filter on $\mathcal{M}(\mathbb{T})$,
- measurements $y \in \mathrm{Im}(\Phi)$.

Agnostic recovery for (BPC). Uniqueness.

Assumption :

- Φ ideal low pass filter on $\mathcal{M}(\mathbb{T})$,
- measurements $y \in \mathrm{Im}(\Phi)$.

Proposition

The matrix

$$T_y = \begin{pmatrix} y_0 & y_1 & \cdots & \cdots & y_{f_c} \\ y_{-1} & y_0 & y_1 & \cdots & y_{f_c-1} \\ \vdots & \ddots & \ddots & \ddots & \vdots \\ y_{-f_c+1} & \cdots & y_{-1} & y_0 & y_1 \\ y_{-f_c} & \cdots & \cdots & y_{-1} & y_0 \end{pmatrix} \in \mathbb{C}^{(f_c+1)\times(f_c+1)}$$

is Toeplitz and hermitian symmetric. Moreover,

$$T_y = V_{x_0} D_{a_0} V_{x_0}^* \quad \Leftrightarrow \quad y = \Phi(m_{a_0,x_0}).$$

where V_{x_0} Vandermonde matrix whose k-th column is $(1 \ e^{ix_{0,k}} \ \cdots \ e^{if_c x_{0,k}})$, D_{a_0} diagonal matrix with a_0 on diagonal.

Agnostic recovery for (BPC). Uniqueness.

Proposition (Carathéodory-Féjer-Pisarenko decomposition)

T_y positive semi-definite and $\mathrm{rank}(T_y) < f_c + 1$.
Then $T_y = V_{x_0} D_{a_0} V_{x_0}^*$ with $(x_0, a_0) \in \mathbb{T}^{\mathrm{rank}(T_y)} \times \mathbb{R}_{>0}^{\mathrm{rank}(T_y)}$ ***unique****.*

Equivalently : T_y positive semi-definite and $\mathrm{rank}(T_y) < f_c + 1$ then $y = \Phi(m_{a_0,x_0})$ with m_{a_0,x_0} unique $\mathrm{rank}(T_y)$-sparse positive measure.

Problem : m_{a_0,x_0} has also lowest TV ?

Agnostic recovery for (BPC). Uniqueness.

Proposition (Carathéodory-Féjer-Pisarenko decomposition)

T_y positive semi-definite and $\mathrm{rank}(T_y) < f_c + 1$.
Then $T_y = V_{x_0} D_{a_0} V_{x_0}^*$ with $(x_0, a_0) \in \mathbb{T}^{\mathrm{rank}(T_y)} \times \mathbb{R}_{>0}^{\mathrm{rank}(T_y)}$ ***unique****.*

Equivalently : T_y positive semi-definite and $\mathrm{rank}(T_y) < f_c + 1$ then $y = \Phi(m_{a_0,x_0})$ with m_{a_0,x_0} unique $\mathrm{rank}(T_y)$-sparse positive measure.

Problem : m_{a_0,x_0} has also lowest TV ?

Theorem (Debarre, D., Fageot 22')

Solutions of (BPC) can be characterized as follows :

1. *If T_y has at least one negative and one positive eigenvalue, then unique solution with at most $2f_c$ Dirac masses, with at least one positive and one negative weight ;*
2. *If T_y is positive, resp. negative, semi-definite and $\mathrm{rank}(T_y) < f_c + 1$, then unique solution with $\mathrm{rank}(T_y)$ positive, resp. negative, Dirac masses ;*
3. *If T_y is positive, resp. negative, definite, then infinitely many solutions, none with less than $f_c + 1$ Dirac masses and uncountably many with $f_c + 1$ positive, resp. negative, Dirac masses.*

Sparse super-resolution of 1D positive measures

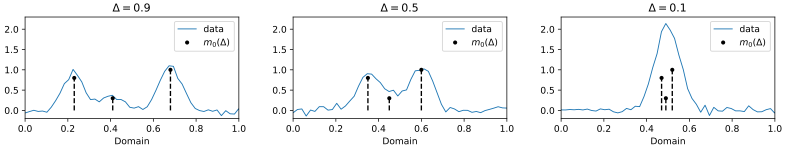

FIGURE – Super-resolution problem : $m_0(\Delta) = \sum_{n=1}^{N} a_{0,n} \delta_{\bar{x}_0 + \Delta \cdot x_{0,n}}$ with $\Delta \to 0$ and $w \sim \mathcal{N}(0, \sigma^2 \mathrm{Id}_{\mathbb{R}^M})$. Φ convolution by sampled 1D Gaussian.

Question : Link N, Δ, λ and σ, when $\Delta \to 0$, to ensure support recovery ?

A Candidate Certificate for (BPC)

Proposition (Certificate)

$m_{a,x}$ is a solution of (BPC) if there exists $\eta \in \mathcal{C}(\mathcal{X}) \cap \mathrm{Im}(\Phi^*)$ satisfying

$$\forall i, \eta(x_{0,i}) = \mathrm{sign}(a_{0,i}) \quad \textit{and} \quad \|\eta\|_\infty \leq 1.$$

Definition (Vanishing Derivatives Pre-certificate - Duval & Peyré 13')

We define p_V as

$$p_V = \mathrm{argmin}\{\|p\| : \forall i = 1, \ldots, N, \ (\Phi^* p)(x_{0,i}) = \mathrm{sign}(a_{0,i}), (\Phi^* p)'(x_{0,i}) = 0\}.$$

p_V is easy to compute. We define the vanishing derivatives pre-certificate as $\eta_V \overset{\text{def.}}{=} \Phi^* p_V$.

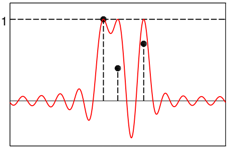

(a) η_V Dirichlet $f_c = 11$

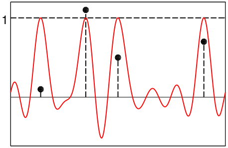

(b) η_V Dirichlet $f_c = 9$

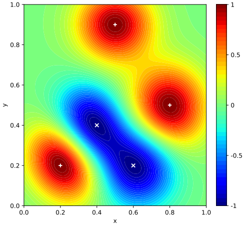

(c) η_V Gaussian 2D

Robustness to Noise of the Support

Theorem (Duval & Peyré 13')

If η_V is non-degenerate i.e.

$$\forall u \in \mathcal{X} \setminus \cup_i \{x_{0,i}\}, |\eta_V(u)| < 1 \quad \text{and} \quad \forall i, \eta_V''(x_{0,i}) \neq 0,$$

then m_{a_0,x_0} unique solution of (BPC) and for all (λ, w) s.t. $\max(\frac{\|w\|}{\lambda}, \lambda) \leq C$ for some $C > 0$, the $(BLASSO)$ has a unique solution $m_{a,x} = \sum_{i=1}^N a_i \delta_{x_i}$ s.t.

$$|(a,x) - (a_0,x_0)|_\infty = O(\lambda, \|w\|).$$

Limit of η_V when $\Delta \to 0$

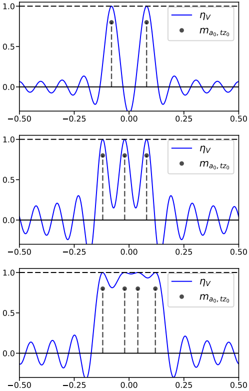

$\Delta = 0.4$

Limit of η_V when $\Delta \to 0$

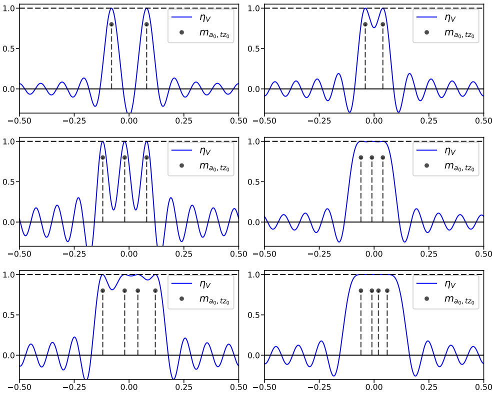

$\Delta = 0.4$ $\Delta = 0.1$

Limit of η_V when $\Delta \to 0$

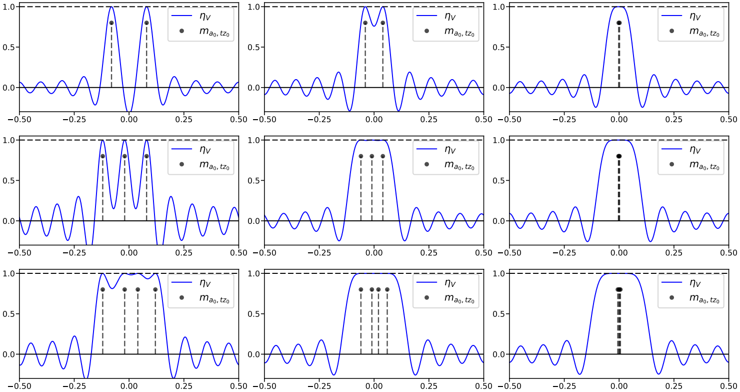

$\Delta = 0.4$ $\Delta = 0.1$ $\Delta = 0.01$

Consequence : η_V converges towards some function η_W satisfying :

- $\eta_W(0) = 1$,
- $\eta_W^{(i)}(0) = 0$ for $1 \leq i \leq 2N - 1$,
- some minimal norm property.

Definition of η_W - D., Duval & Peyré 17'

Definition ((2$N-1$)-Vanishing Derivatives Pre-certificate)

We define p_W as

$$p_W = \textit{argmin}\{\|p\| : (\Phi^* p)(0) = 1, (\Phi^* p)'(0) = 0, \dots, (\Phi^* p)^{(2N-1)}(0) = 0\}.$$

We define the $(2N-1)$-vanishing derivatives pre-certificate as $\eta_W \stackrel{\text{def.}}{=} \Phi^* p_W$.

Definition of η_W - D., Duval & Peyré 17'

Definition ((2$N-1$)-Vanishing Derivatives Pre-certificate)

We define p_W as

$$p_W = \text{argmin}\{\|p\| : (\Phi^* p)(0) = 1, (\Phi^* p)'(0) = 0, \dots, (\Phi^* p)^{(2N-1)}(0) = 0\}.$$

We define the $(2N-1)$*-vanishing derivatives pre-certificate as* $\eta_W \overset{\text{def.}}{=} \Phi^* p_W$.

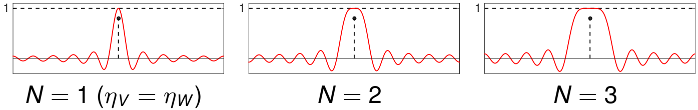

FIGURE – η_W for several value of N, where Φ is the ideal low-pass filter.

Definition of η_W - D., Duval & Peyré 17'

Definition ($(2N-1)$-Vanishing Derivatives Pre-certificate)

We define p_W as

$$p_W = \mathrm{argmin}\{\|p\| :\ (\Phi^* p)(0) = 1, (\Phi^* p)'(0) = 0, \ldots, (\Phi^* p)^{(2N-1)}(0) = 0\}.$$

We define the $(2N-1)$-vanishing derivatives pre-certificate as $\eta_W \overset{\text{def.}}{=} \Phi^* p_W$.

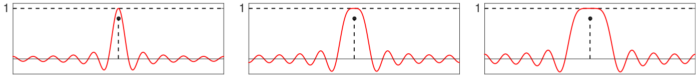

$N = 1$ $(\eta_V = \eta_W)$ $\qquad$ $N = 2$ $\qquad$ $N = 3$

FIGURE – η_W for several value of N, where Φ is the ideal low-pass filter.

Intuition : the behavior of η_V is therefore governed by specific properties of η_W for small values of $\Delta > 0$.

Definition of η_W - D., Duval & Peyré 17'

Definition ((2N – 1)-Vanishing Derivatives Pre-certificate)

We define p_W as

$$p_W = \text{argmin}\{\|p\| : \ (\Phi^* p)(0) = 1, (\Phi^* p)'(0) = 0, \ldots, (\Phi^* p)^{(2N-1)}(0) = 0\}.$$

We define the $(2N-1)$-vanishing derivatives pre-certificate as $\eta_W \overset{\text{def.}}{=} \Phi^* p_W$.

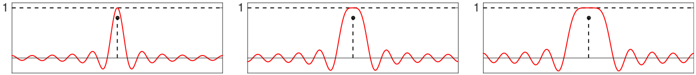

$N = 1$ ($\eta_V = \eta_W$) $N = 2$ $N = 3$

FIGURE – η_W for several value of N, where Φ is the ideal low-pass filter.

Intuition : the behavior of η_V is therefore governed by specific properties of η_W for small values of $\Delta > 0$.

Definition (Non-Degeneracy of η_W)

η_W is $(2N-1)$-non-degenerate if :

$$\eta_W^{(2N)}(0) \neq 0 \quad \textit{and} \quad \forall u \in \mathcal{X} \setminus \{0\}, |\eta_W(u)| < 1.$$

Separation Influence on Robustness of Super-Resolution

Theorem (D., Duval & Peyré 17')

If η_W *is* $(2N-1)$*-non-degenerate, there exist* $\Delta_0 > 0$*,* $C_R > 0$*,* $C > 0$ *and* $M > 0$ *which depend only on* Φ *and* (a_0, z_0) *such that*

$$\forall t \in (0, \Delta_0)\,, \quad \forall (\lambda, w) \in B(0, C_R \Delta^{2N-1}) \quad \text{and} \quad \left\| \frac{w}{\lambda} \right\| \leq C,$$

the problem $(BLASSO)$ *admits a unique solution* $m_{a,tz}$ *composed of exactly* N *spikes and* $m_{a,tz}$ *satisfies :*

$$|(a, z) - (a_0, z_0)|_\infty \leq M \left(\frac{|\lambda|}{\Delta^{2N-1}} + \frac{\|w\|}{\Delta^{2N-1}} \right).$$

Separation Influence on Robustness of Super-Resolution

Theorem (D., Duval & Peyré 17')

If η_W is $(2N-1)$-non-degenerate, there exist $\Delta_0 > 0$, $C_R > 0$, $C > 0$ and $M > 0$ which depend only on Φ and (a_0, z_0) such that

$$\forall t \in (0, \Delta_0)\,, \quad \forall(\lambda, w) \in B(0, C_R \Delta^{2N-1}) \quad \text{and} \quad \left\| \frac{w}{\lambda} \right\| \leq C,$$

the problem (BLASSO) admits a unique solution $m_{a,tz}$ composed of exactly N spikes and $m_{a,tz}$ satisfies :

$$|(a, z) - (a_0, z_0)|_\infty \leq M \left(\frac{|\lambda|}{\Delta^{2N-1}} + \frac{\|w\|}{\Delta^{2N-1}} \right).$$

Optimality of the scaling of w and λ in Δ^{2N-1}

Suppose that $w = \lambda w_0$ and $\lambda = \Delta^\alpha \lambda_0$.

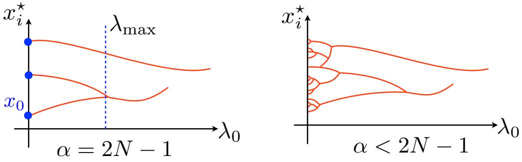

Grid-less algorithm for BLASSO

Goal : solve numerically (BLASSO)

$$\min_{m \in \mathcal{M}} \frac{1}{2} \|\Phi m - y\|_2^2 + \lambda \|m\|_{\mathcal{M}}$$

Several approaches :

- discretization : LASSO $\rightarrow$ FISTA,
- SDP formulation (only for Fourier measurements), [Candes-FG 13', Catala & al. 19'],

Grid-less algorithm for BLASSO

Goal : solve numerically (BLASSO)

$$\min_{m \in \mathcal{M}} \frac{1}{2} \|\Phi m - y\|_2^2 + \lambda \|m\|_{\mathcal{M}}$$

Several approaches :

- discretization : LASSO $\rightarrow$ FISTA,
- SDP formulation (only for Fourier measurements), [Candes-FG 13', Catala & al. 19'],
- solve (BLASSO) on Banach space $\mathcal{M}(\mathcal{X}) \rightarrow$ **Frank-Wolfe algorithm**, [Bredies & al '13, Boyd & al '17].

Frank-Wolfe algorithm

FW applies to

$$\min_{m \in C} f(m),$$

- C weakly-compact convex set of Banach space,
- f differentiable with Lipschitz gradient.

The algorithm :

for $k = 0, \dots, n$ **do**

  Minimize : $s_k \in \mathrm{argmin}_{s \in C} f(m_k) + df(m_k)[s - m_k]$.

  if $df(m_k)[s_k - m_k] = 0$ **then**

    m_k solution. Stop.

  else

    Step research : $\gamma_k \leftarrow \frac{2}{k+2}$ or $\gamma_k \in \mathrm{argmin}_{\gamma \in [0,1]} f(m_k + \gamma(s_k - m_k))$.

    Update : $m_{k+1} \leftarrow m_k + \gamma_k(s_k - m_k)$.

  end if

end for

The Sliding Frank-Wolfe Algorithm [D., Duval & Peyré]

Start with $m_0 = 0$.

The Sliding Frank-Wolfe Algorithm [D., Duval & Peyré]

Start with $m_0 = 0$.

2: **for** $k = 0, \ldots, n$ **do**

$m_k = \sum_{i=1}^{N_k} a_i^k \delta(\cdot - x_i^k)$, $a_i^k \in \mathbb{R}$, $x_i^k \in \mathcal{X}$. Find

$$\boxed{x_*^k \in \underset{x \in \mathcal{X}}{\operatorname{argmax}} |\eta_k(x)| \quad \text{where} \quad \eta_k \overset{\text{def.}}{=} \frac{1}{\lambda}\Phi^*(y - \Phi m_k) \in \mathcal{C}_0(\mathcal{X}),}$$

Step 1 : add new Dirac mass (non-convex)

The Sliding Frank-Wolfe Algorithm [D., Duval & Peyré]

Start with $m_0 = 0$.

for $k = 0, \dots, n$ **do**

$m_k = \sum_{i=1}^{N_k} a_i^k \delta(\cdot - x_i^k)$, $a_i^k \in \mathbb{R}$, $x_i^k \in \mathcal{X}$. Find

$$\boxed{x_*^k \in \underset{x \in \mathcal{X}}{\operatorname{argmax}} |\eta_k(x)| \quad \text{where} \quad \eta_k \overset{\text{def.}}{=} \frac{1}{\lambda}\Phi^*(y - \Phi m_k) \in \mathcal{C}_0(\mathcal{X}),}$$

Step 1 : add new Dirac mass (non-convex)

if $|\eta_k(x_*^k)| \leq 1$ **then**

m_k solution of (BLASSO). Stop.

The Sliding Frank-Wolfe Algorithm [D., Duval & Peyré]

Start with $m_0 = 0$.

for $k = 0, \dots, n$ **do**

$m_k = \sum_{i=1}^{N_k} a_i^k \delta(\cdot - x_i^k)$, $a_i^k \in \mathbb{R}$, $x_i^k \in \mathcal{X}$. Find

$$\boxed{x_*^k \in \operatorname*{argmax}_{x \in \mathcal{X}} |\eta_k(x)| \quad \text{where} \quad \eta_k \overset{\text{def.}}{=} \frac{1}{\lambda} \Phi^*(y - \Phi m_k) \in \mathcal{C}_0(\mathcal{X}),}$$

Step 1 : add new Dirac mass (non-convex)

if $|\eta_k(x_*^k)| \leq 1$ **then**

m_k solution of (BLASSO). Stop.

else

Find

$$\boxed{\begin{aligned} (a_i^{k+1/2})_{1 \leq i \leq N_k+1} \ni \operatorname*{argmin}_{a \in \mathbb{R}^{N_k+1}} \frac{1}{2} \|\Phi_{\mathcal{G}} a - y\|_2^2 + \lambda \|a\|_1 \, , \\ \text{where} \quad \mathcal{G} = (x_1^k, \dots, x_{N_k}^k, x_*^k). \end{aligned}}$$

Step 2 : compute new weights (convex, LASSO)

The Sliding Frank-Wolfe Algorithm [D., Duval & Peyré]

Start with $m_0 = 0$.

for $k = 0, \ldots, n$ **do**

$m_k = \sum_{i=1}^{N_k} a_i^k \delta(\cdot - x_i^k)$, $a_i^k \in \mathbb{R}$, $x_i^k \in \mathcal{X}$. Find

$$x_*^k \in \underset{x \in \mathcal{X}}{\operatorname{argmax}} |\eta_k(x)| \quad \text{where} \quad \eta_k \overset{\text{def.}}{=} \frac{1}{\lambda}\Phi^*(y - \Phi m_k) \in \mathcal{C}_0(\mathcal{X}),$$

Step 1 : add new Dirac mass (non-convex)

if $|\eta_k(x_*^k)| \leq 1$ **then**

m_k solution of (BLASSO). Stop.

else

Find

$$(a_i^{k+1/2})_{1 \leq i \leq N_k+1} \ni \underset{a \in \mathbb{R}^{N_k+1}}{\operatorname{argmin}} \frac{1}{2} \|\Phi_{\mathcal{G}} a - y\|_2^2 + \lambda \|a\|_1 ,$$

$$\text{where} \quad \mathcal{G} = (x_1^k, \ldots, x_{N_k}^k, x_*^k).$$

Step 2 : compute new weights (convex, LASSO)

Initialize with $((a_i^{k+1/2})_{1 \leq i \leq N_k+1}, \mathcal{G})$. Find

$$((a_i^{k+1}), (x_i^{k+1})) \ni \underset{(a,x) \in \mathbb{R}^{N_k+1} \times \mathcal{X}^{N_k+1}}{\operatorname{argmin}} \frac{1}{2} \|\Phi_x a - y\|_2^2 + \lambda \|a\|_1 .$$

Step 3 : local descent (non-convex)

end if

end for

Illustration of the algorithm : 2D SMLM example

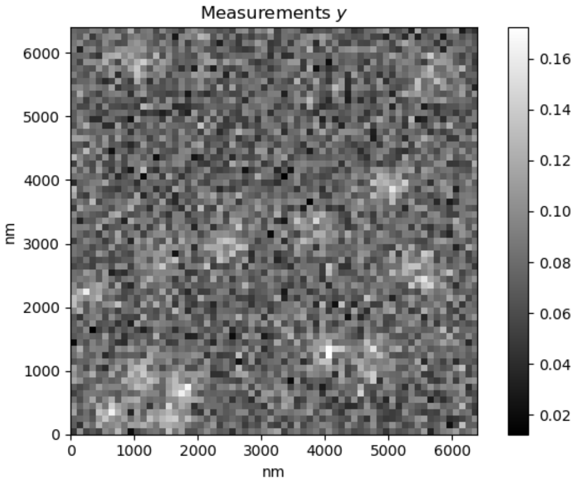

FIGURE – One frame of a sequence of SMLM acquisitions. PSF : integration over pixel domain of 2D Gaussian convolution (width 200nm). Background noise + Gaussian noise

Illustration of the algorithm : 2D SMLM example

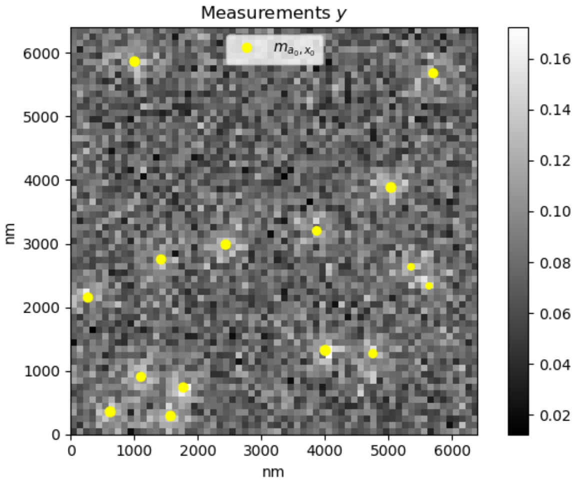

FIGURE – One frame of a sequence of SMLM acquisitions. PSF : integration over pixel domain of 2D Gaussian convolution (width 200nm). Background noise + Gaussian noise

Illustration of the algorithm : 2D SMLM example

Iteration 9

$$\eta_k = \frac{1}{\lambda}\Phi^*(y - \Phi(m_k))$$

Measures $m_{k+1/2}$ and m_k

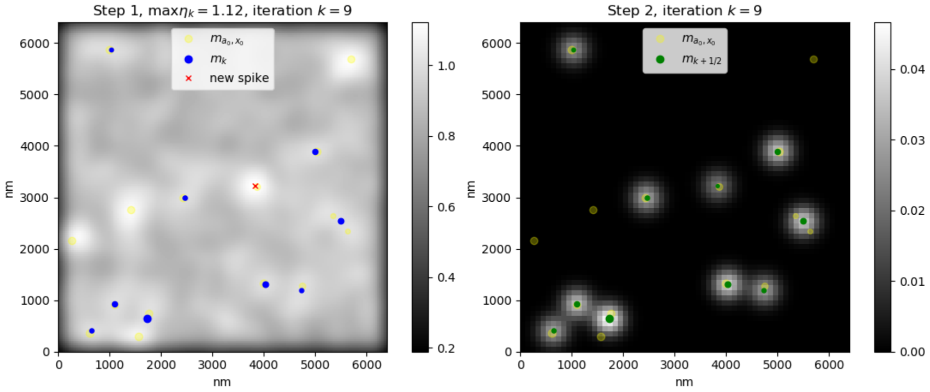

FIGURE – Main steps of the SFW algorithm.

Illustration of the algorithm : 2D SMLM example

Iteration 9

$$\eta_k = \frac{1}{\lambda}\Phi^*(y - \Phi(m_k))$$

Measures $m_{k+1/2}$ and m_k

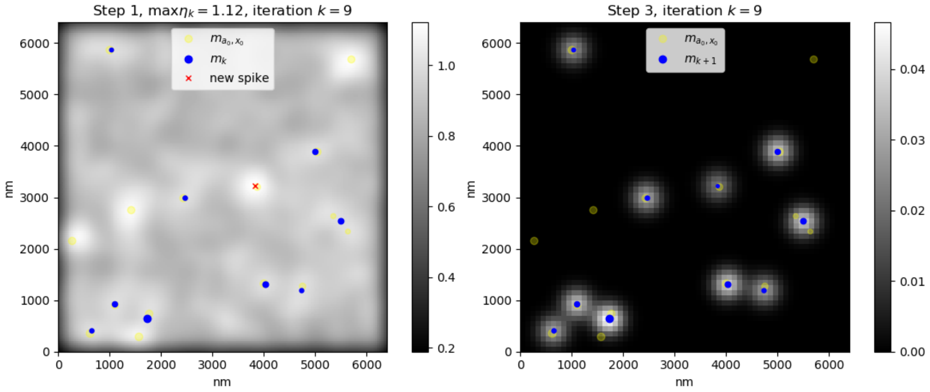

FIGURE – Main steps of the SFW algorithm.

Illustration of the algorithm : 2D SMLM example

Iteration 10

$\eta_k = \frac{1}{\lambda}\Phi^*(y - \Phi(m_k))$ Measures $m_{k+1/2}$ and m_k

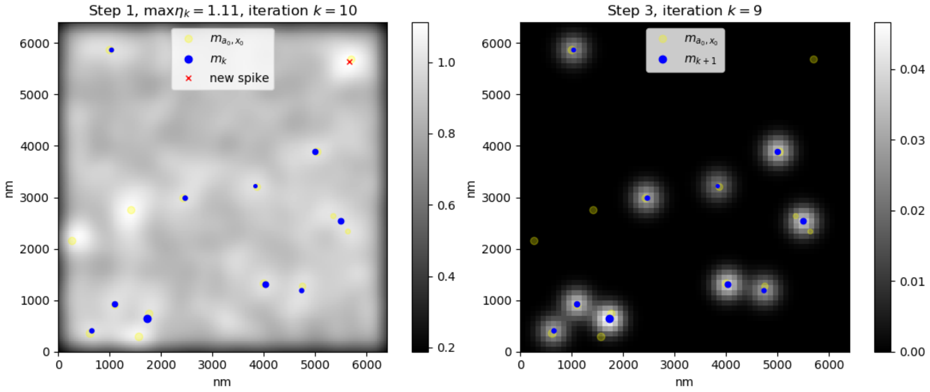

FIGURE – Main steps of the SFW algorithm.

Illustration of the algorithm : 2D SMLM example

Iteration 10

$\eta_k = \frac{1}{\lambda}\Phi^*(y - \Phi(m_k))$

Measures $m_{k+1/2}$ and m_k

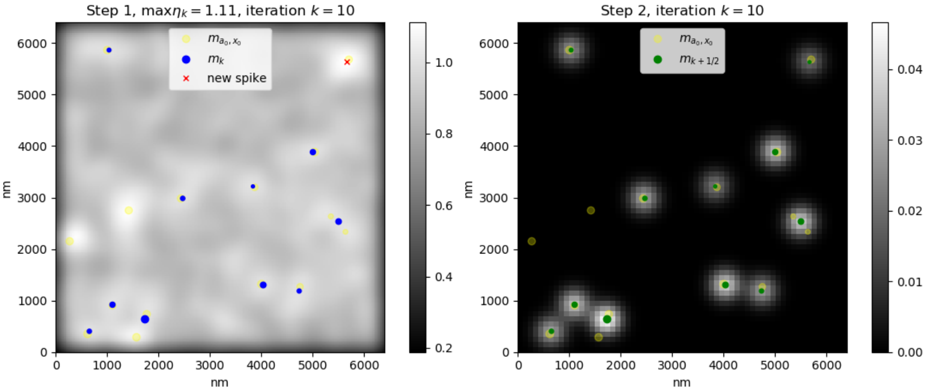

FIGURE – Main steps of the SFW algorithm.

Illustration of the algorithm : 2D SMLM example

Iteration 10

$$\eta_k = \frac{1}{\lambda}\Phi^*(y - \Phi(m_k))$$

Measures $m_{k+1/2}$ and m_k

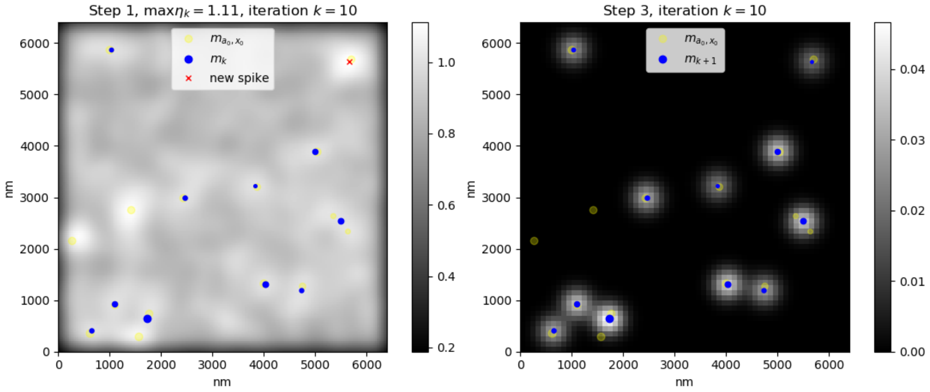

FIGURE – Main steps of the SFW algorithm.

Illustration of the algorithm : 2D SMLM example

Iteration 11

$$\eta_k = \frac{1}{\lambda}\Phi^*(y - \Phi(m_k))$$

Measures $m_{k+1/2}$ and m_k

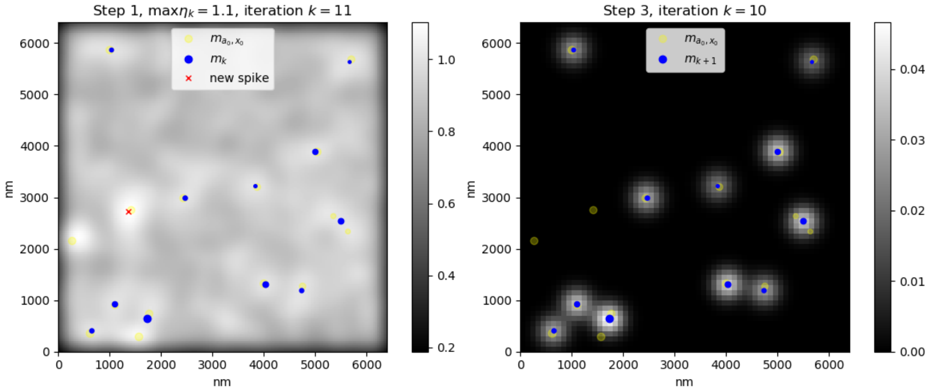

FIGURE – Main steps of the SFW algorithm.

Illustration of the algorithm : 2D SMLM example

Iteration 11

$\eta_k = \frac{1}{\lambda}\Phi^*(y - \Phi(m_k))$ Measures $m_{k+1/2}$ and m_k

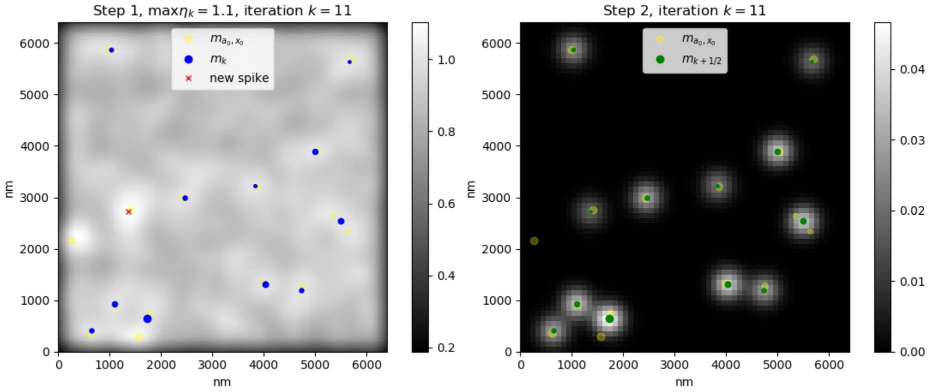

FIGURE – Main steps of the SFW algorithm.

Illustration of the algorithm : 2D SMLM example

Iteration 11

$$\eta_k = \frac{1}{\lambda}\Phi^*(y - \Phi(m_k))$$

Measures $m_{k+1/2}$ and m_k

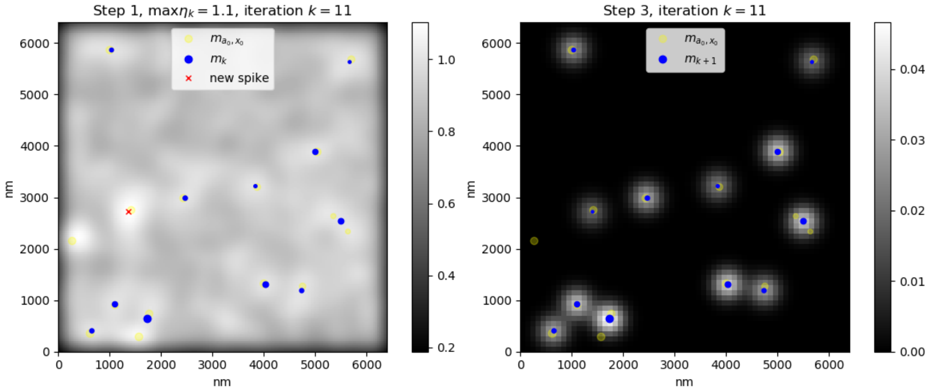

FIGURE – Main steps of the SFW algorithm.

Illustration of the algorithm : 2D SMLM example

Iteration 12

$$\eta_k = \frac{1}{\lambda}\Phi^*(y - \Phi(m_k))$$

Measures $m_{k+1/2}$ and m_k

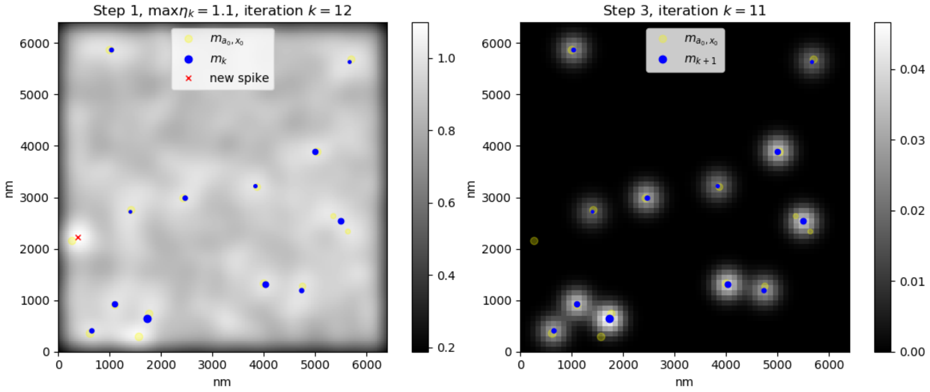

FIGURE – Main steps of the SFW algorithm.

Illustration of the algorithm : 2D SMLM example

Iteration 12

$$\eta_k = \frac{1}{\lambda}\Phi^*(y - \Phi(m_k))$$

Measures $m_{k+1/2}$ and m_k

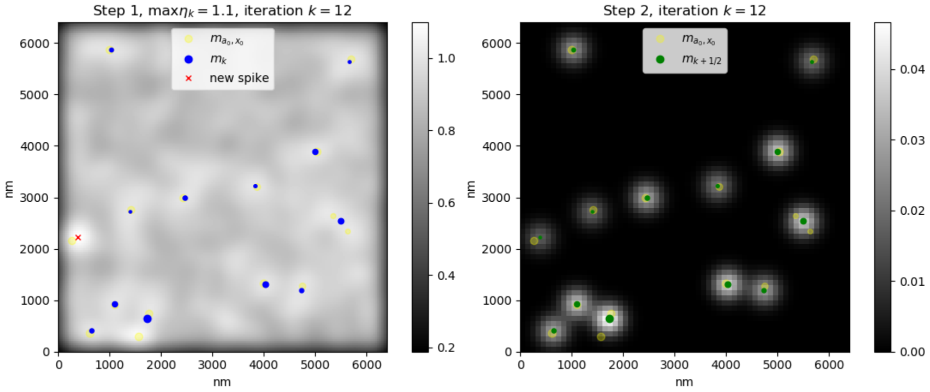

FIGURE – Main steps of the SFW algorithm.

Illustration of the algorithm : 2D SMLM example

Iteration 12

$$\eta_k = \frac{1}{\lambda}\Phi^*(y - \Phi(m_k))$$

Measures $m_{k+1/2}$ and m_k

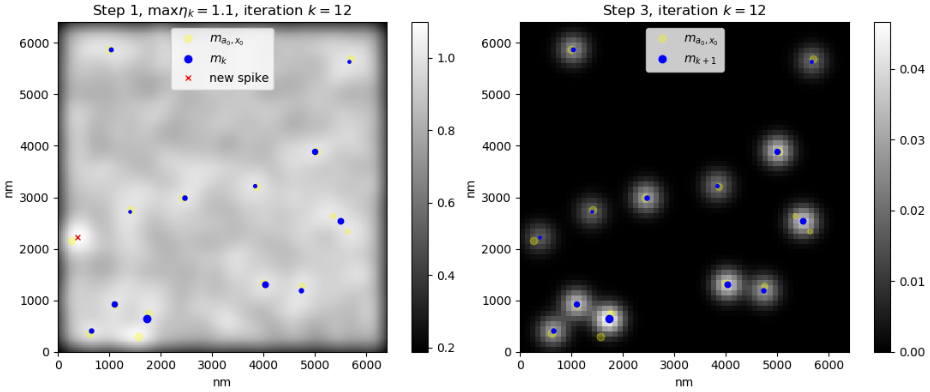

FIGURE – Main steps of the SFW algorithm.

Illustration of the algorithm : 2D SMLM example

Iteration 13

$$\eta_k = \frac{1}{\lambda}\Phi^*(y - \Phi(m_k))$$

Measures $m_{k+1/2}$ and m_k

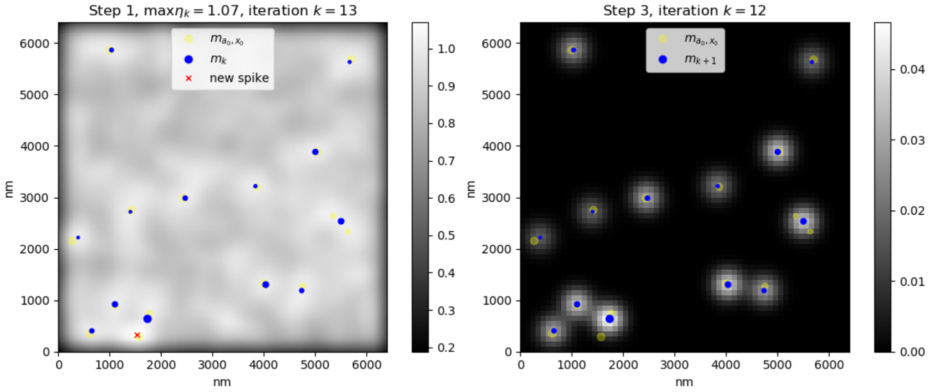

FIGURE – Main steps of the SFW algorithm.

Illustration of the algorithm : 2D SMLM example

Iteration 13

$\eta_k = \frac{1}{\lambda}\Phi^*(y - \Phi(m_k))$

Measures $m_{k+1/2}$ and m_k

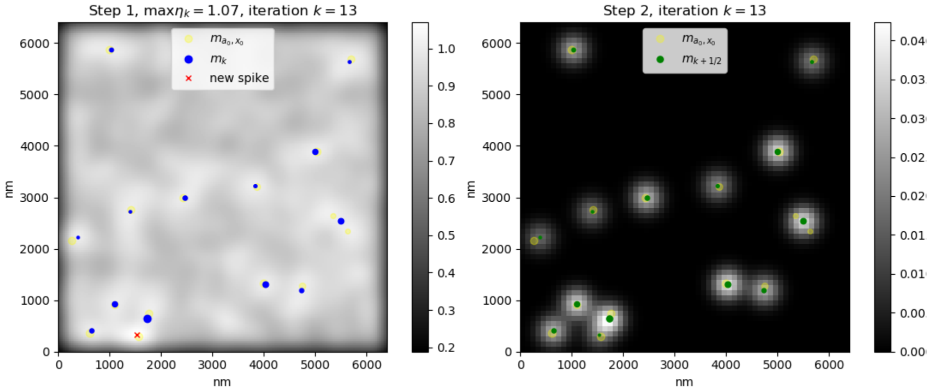

FIGURE – Main steps of the SFW algorithm.

Illustration of the algorithm : 2D SMLM example

Iteration 13

$\eta_k = \frac{1}{\lambda}\Phi^*(y - \Phi(m_k))$

Measures $m_{k+1/2}$ and m_k

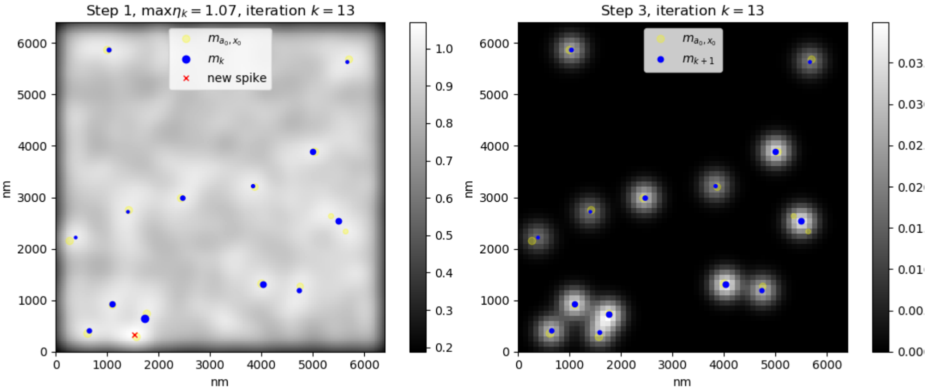

FIGURE – Main steps of the SFW algorithm.

Illustration of the algorithm : 2D SMLM example

Iteration 14

$$\eta_k = \frac{1}{\lambda}\Phi^*(y - \Phi(m_k))$$

Measures $m_{k+1/2}$ and m_k

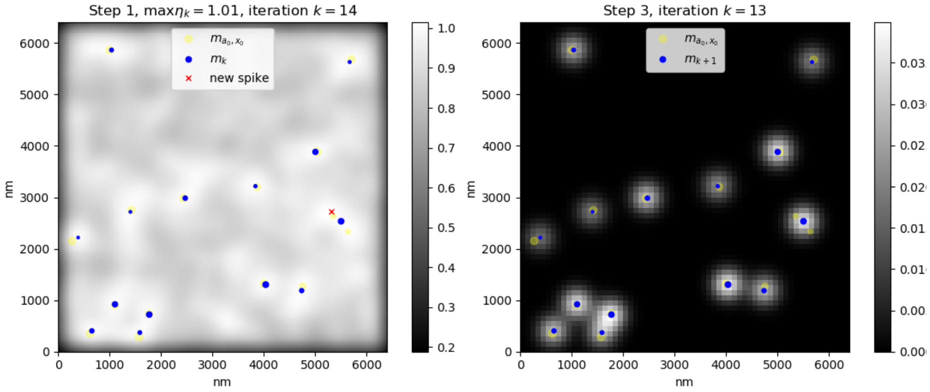

FIGURE – Main steps of the SFW algorithm.

Illustration of the algorithm : 2D SMLM example

Iteration 14

$\eta_k = \frac{1}{\lambda}\Phi^*(y - \Phi(m_k))$

Measures $m_{k+1/2}$ and m_k

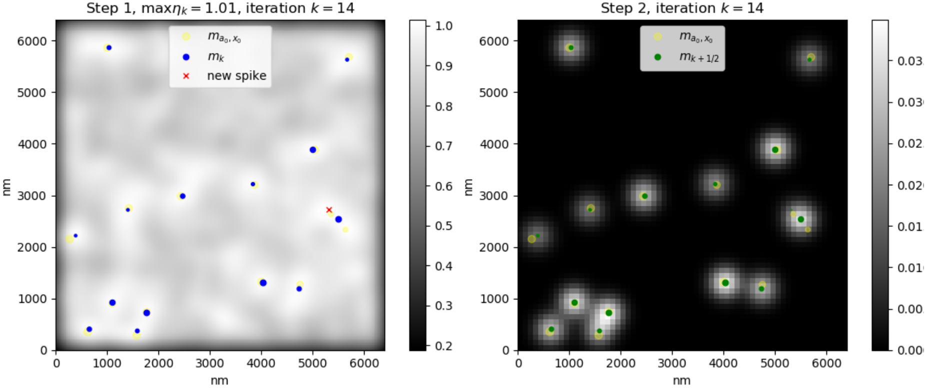

FIGURE – Main steps of the SFW algorithm.

Illustration of the algorithm : 2D SMLM example

Iteration 14

$$\eta_k = \frac{1}{\lambda}\Phi^*(y - \Phi(m_k))$$

Measures $m_{k+1/2}$ and m_k

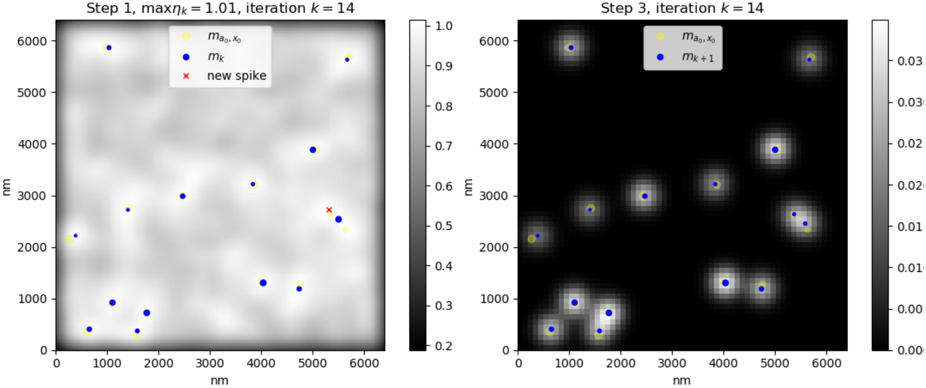

FIGURE – Main steps of the SFW algorithm.

Illustration of the algorithm : 2D SMLM example

Iteration 15

$\eta_k = \frac{1}{\lambda}\Phi^*(y - \Phi(m_k))$

Stopping criteria

Measures $m_{k+1/2}$ and m_k

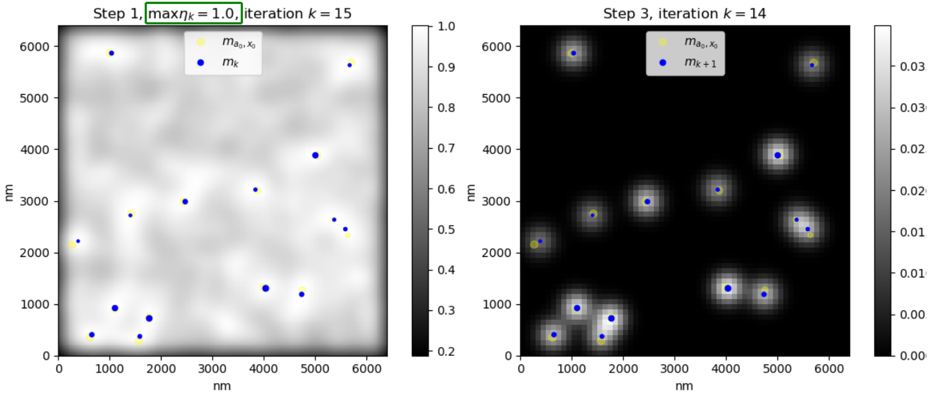

FIGURE – Main steps of the SFW algorithm.

Convergence of the algorithm in 15 main iterations.

Finite Time Convergence of the SFW

Theorem (D., Duval & Peyré)

Suppose $m_{a,x} = \sum_{i=1}^{N} a_i \delta_{x_i}$ *unique solution of (BLASSO) and* $\eta_\lambda = \frac{1}{\lambda}\Phi^*(y - \Phi m_{a,x})$ *is non-degenerate i.e. :*

$$\forall t \in \mathcal{X} \setminus \bigcup_{i=1}^{N} \{x_i\}, \quad |\eta_\lambda(t)| < 1 \quad \textit{and} \quad \forall i \in \{1, \ldots, N\}, \quad \eta_\lambda''(x_i) \neq 0.$$

Then the SFW algorithm recovers $m_{a,x}$ *after finite number of iterations i.e. there exists* $k \in \mathbb{N}$ *such that* $m_k = m_{a,x}$.

Finite Time Convergence of the SFW

Theorem (D., Duval & Peyré)

Suppose $m_{a,x} = \sum_{i=1}^{N} a_i \delta_{x_i}$ *unique solution of (BLASSO) and* $\eta_\lambda = \frac{1}{\lambda}\Phi^*(y - \Phi m_{a,x})$ *is non-degenerate i.e. :*

$$\forall t \in \mathcal{X} \setminus \bigcup_{i=1}^{N} \{x_i\}, \quad |\eta_\lambda(t)| < 1 \quad \textit{and} \quad \forall i \in \{1, \dots, N\}, \quad \eta_\lambda''(x_i) \neq 0.$$

Then the SFW algorithm recovers $m_{a,x}$ *after finite number of iterations i.e. there exists* $k \in \mathbb{N}$ *such that* $m_k = m_{a,x}$.

Open question : convergence in exactly N iterations ?

PALM+MA-TIRF Model (Morpheme team, Institute of Biology Valrose (iBV))

The kernel ϕ of forward operator Φ, where $\Phi m = \int_{\mathcal{X}} \phi(x,y,z)\mathrm{d}m(x,y,z)$, is given by

$$\phi(x,y,z) = (\psi_{xy}(x_i - x)\psi_{xy}(y_i - y)\psi_k(z))_{(i,j,k)\in\{1,\dots,N_p\}^2\times\{1,\dots,K\}} \in \mathbb{R}^{N_p \times N_p \times K}.$$

with for all $s \in \mathbb{R}$, for all $k \in \{1, \dots, K\}$ and for all $z \in [0, z_b]$:

$$\psi_{xy}(s) = \frac{1}{\sqrt{2\pi\sigma^2}} \int_{s-\frac{1}{2N_p}}^{s+\frac{1}{2N_p}} e^{-\frac{u^2}{2\sigma^2}} \mathrm{d}u,$$

$$\psi_k(z) = \xi(z)e^{-s_k z} \quad \text{with} \quad \xi(z) = \left(\sum_{k=1}^{K} e^{-2s_k z}\right)^{-1/2}.$$

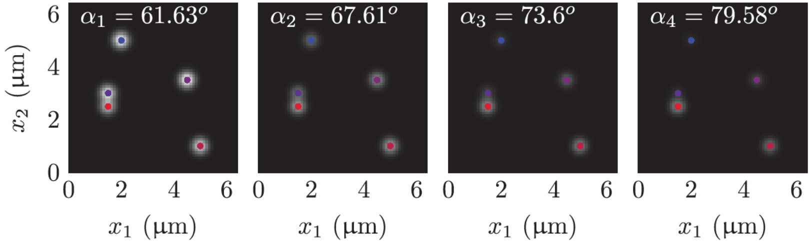

FIGURE – $y_0 = \Phi m_{a_0,\bar{x}_0}$ when $K = 4$ for the PALM+MA-TIRF model and $m_{a_0,\bar{x}_0} = \delta(\cdot - (1.5, 2.5, 0.1)) + \delta(\cdot - (1.5, 3, 0.5)) + \delta(\cdot - (2, 5, 0.7)) + \delta(\cdot - (4.5, 3.5, 0.4)) + \delta(\cdot - (5, 1, 0.2))$.

PALM+Astigmatism Model (Huang & al, '08)

The kernel ϕ of forward operator Φ is given by

$$\phi(x,y,z) = (\psi_{x,k}(x_i - x, z)\psi_{y,k}(y_i - y, z))_{(i,j,k)\in\{1,\dots,N_p\}^2\times\{1,\dots,K\}} \in \mathbb{R}^{N_p\times N_p\times K}.$$

where for all $s \in \mathbb{R}$, for all $z \in [0, z_b]$ and for all $k \in \{1, \dots, K\}$:

$$\psi_{xy}(s) = \frac{1}{\sqrt{2\pi\sigma_{x,k}(z)^2}} \int_{s-\frac{1}{2N_p}}^{s+\frac{1}{2N_p}} e^{-\frac{u^2}{2\sigma_{x,k}(z)^2}} \mathrm{d}u.$$

with :

$$\sigma_{x,k}(z) = \sigma_0\sqrt{1 + \left(\frac{\alpha(z - f_{p,k}) - \beta}{d}\right)^2} \quad \text{and} \quad \sigma_{y,k}(z) = \sigma_{x,k}(-z + 2f_{p,k}).$$

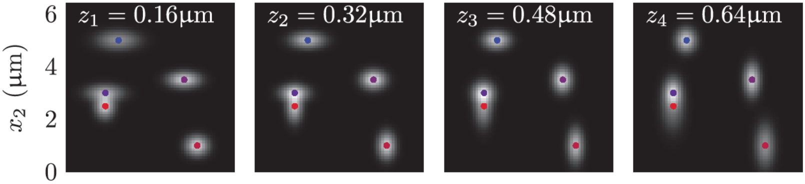

FIGURE – $y_0 = \Phi m_{a_0,\bar{x}_0}$ when $K = 4$ for the PALM+Astigmatism model and $m_{a_0,\bar{x}_0} = \delta(\cdot - (1.5, 2.5, 0.1)) + \delta(\cdot - (1.5, 3, 0.5)) + \delta(\cdot - (2, 5, 0.7)) + \delta(\cdot - (4.5, 3.5, 0.4)) + \delta(\cdot - (5, 1, 0.2))$.

PALM+Double-Helix Model (Pavani & al, '09)

The kernel ϕ of forward operator Φ is given by

$$\phi(x,y,z) = \left(\psi^1_{x,k}(x_i - x, z)\psi^1_{y,k}(y_i - y, z) + \psi^{-1}_{x,k}(x_i - x, z)\psi^{-1}_{y,k}(y_i - y, z)\right)_{(i,j)},$$

with for all $s \in \mathbb{R}$ and for all $z \in [0, z_b]$:

$$\psi_{xy}(s) = \frac{1}{\sqrt{2\pi\sigma^2}} \int_{s-\frac{1}{2N_p}-\varepsilon r_{x,k}(z)}^{s+\frac{1}{2N_p}-\varepsilon r_{x,k}(z)} e^{-\frac{u^2}{2\sigma^2}}\,\mathrm{d}u.$$

where :

$$r_{x,k}(z) = \frac{\omega}{2}\cos(\theta_k(z)), \quad r_{y,k}(z) = -\frac{\omega}{2}\sin(\theta_k(z)) \quad \text{and} \quad \theta_k(z) = \frac{\pi}{3}\frac{z - f_{p,k}}{f_{p,K}}.$$

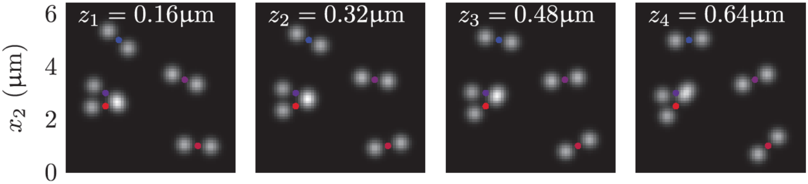

FIGURE – $y_0 = \Phi m_{a_0,\bar{x}_0}$ when $K = 4$ for the PALM+Double-Helix model and $m_{a_0,\bar{x}_0} = \delta(\cdot - (1.5, 2.5, 0.1)) + \delta(\cdot - (1.5, 3, 0.5)) + \delta(\cdot - (2, 5, 0.7)) + \delta(\cdot - (4.5, 3.5, 0.4)) + \delta(\cdot - (5, 1, 0.2))$.

Comparison of different acquisition modalities for 3D SMLM

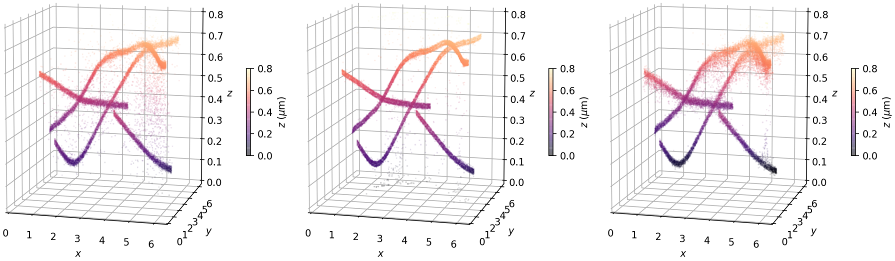

(a) Astigmatism (b) Double Helix (c) MA-TIRF

FIGURE – Recovered tubular structures (width : 20nm) from different 3D acquisition modalities and synthetic data. Acquisition : 20k frames with $\simeq$ 10 fluorophores per frame.

Sparse piecewise linear representation of data (Debarre, D., Fageot, Unser 21')

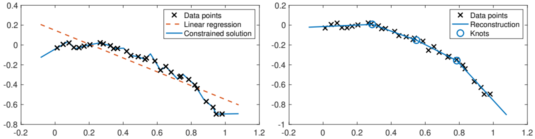

FIGURE – Sparse piecewise linear interpolation

Sparse piecewise linear representation of data (Debarre, D., Fageot, Unser 21')

Exact interpolation :

$$\min_{f \in \mathcal{M}_{\mathrm{D}^2}, f(x_m) = y_{0,m}} \left\| \mathrm{D}^2 f \right\|_{\mathcal{M}} \quad \text{where} \quad \mathcal{M}_{\mathrm{D}^2} \stackrel{\text{def.}}{=} \{ f \in \mathcal{S}'(\mathbb{R}) : \ \mathrm{D}^2 f \in \mathcal{M} \}.$$

Existence of sparse solutions :

$$\forall t \in \mathbb{R}, \quad f_\star(t) = \left((\cdot)_+ * m_{a_0, x_0} \right)(t) + \alpha + \beta t.$$

Sparse piecewise linear representation of data (Debarre, D., Fageot, Unser 21')

Exact interpolation :

$$\min_{f \in \mathcal{M}_{\mathrm{D}^2}, f(x_m)=y_{0,m}} \left\|\mathrm{D}^2 f\right\|_{\mathcal{M}} \quad \text{where} \quad \mathcal{M}_{\mathrm{D}^2} \stackrel{\text{def.}}{=} \{f \in \mathcal{S}'(\mathbb{R}) : \ \mathrm{D}^2 f \in \mathcal{M}\}.$$

Existence of sparse solutions :

$$\forall t \in \mathbb{R}, \quad f_\star(t) = ((\cdot)_+ * m_{a_0, x_0})(t) + \alpha + \beta t.$$

Key idea : dual certificates also piecewise linear $\eta = \sum_{m=1}^{M} c_m \, (x_m - \cdot)_+$.

Sparse piecewise linear representation of data (Debarre, D., Fageot, Unser 21')

Exact interpolation :

$$\min_{f \in \mathcal{M}_{\mathrm{D}^2}, f(x_m)=y_{0,m}} \left\| \mathrm{D}^2 f \right\|_{\mathcal{M}} \quad \text{where} \quad \mathcal{M}_{\mathrm{D}^2} \overset{\text{def.}}{=} \{ f \in \mathcal{S}'(\mathbb{R}) : \ \mathrm{D}^2 f \in \mathcal{M} \}.$$

Existence of sparse solutions :

$$\forall t \in \mathbb{R}, \quad f_\star(t) = ((\cdot)_+ * m_{a_0,x_0})(t) + \alpha + \beta t.$$

Key idea : dual certificates also piecewise linear $\eta = \sum_{m=1}^{M} c_m \, (x_m - \cdot)_+$.

Consequences :

- *connecting the data points* gives solution. $f_{\text{cano}} = a_1 + a_M t + \sum_{m=2}^{M-1} a_m(\cdot - x_m)_+$

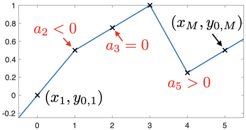

Canonical solution

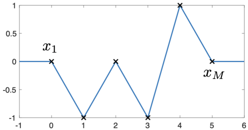

Canonical certificate

Sparse piecewise linear representation of data (Debarre, D., Fageot, Unser 21')

Exact interpolation :

$$\min_{f \in \mathcal{M}_{\mathrm{D}^2}, f(x_m)=y_{0,m}} \left\|\mathrm{D}^2 f\right\|_{\mathcal{M}} \quad \text{where} \quad \mathcal{M}_{\mathrm{D}^2} \stackrel{\text{def.}}{=} \{f \in \mathcal{S}'(\mathbb{R}) : \ \mathrm{D}^2 f \in \mathcal{M}\}.$$

Existence of sparse solutions :

$$\forall t \in \mathbb{R}, \quad f_\star(t) = \left((\cdot)_+ * m_{a_0,x_0}\right)(t) + \alpha + \beta t.$$

Key idea : dual certificates also piecewise linear $\eta = \sum_{m=1}^{M} c_m (x_m - \cdot)_+$.

Consequences :

- *connecting the data points* gives solution. $f_{\text{cano}} = a_1 + a_M t + \sum_{m=2}^{M-1} a_m(\cdot - x_m)_+$

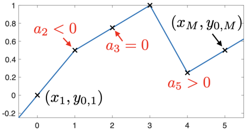

Canonical solution

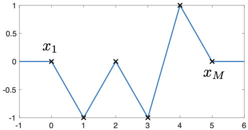

Canonical certificate

- getting sparsest solutions in $O(M)$ operations,

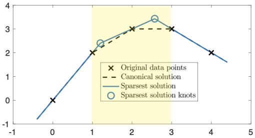

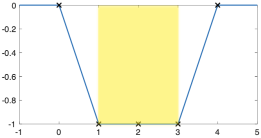

Conclusion

Summary :

- many problems can be formulated as sparse inverse problems over continuous domain ;
- strong theoretical guarentees : existence, uniqueness, robustness to noise, super-resolution... ;
- existence of solvers that work in the continuum with convergence guarentees ;
- extensions to generalized TV (TV with differential operators).

Challenges :

- dimension $d > 1$ harder to analyse theoretically ;
- sliding step becomes slow when dealing with lots of Dirac masses (see Courbot & al 21' for an acceleration).

Merci de votre attention.